Received: 22 December 2023 | Revised: 14 March 2024 | Accepted: 19 March 2024

DOI: 10.1002/mp.17045

RESEARCH ARTICLE

MEDICAL PHYSICS

Robustness of carbon-ion radiotherapy against DNA damage repair associated radiosensitivity variation based on a biophysical model

Hans Liew[1,2,3] | **Thomas Tessonnier**[4,5] | **Stewart Mein**[1,2,3,6] | **Giuseppe Magro**[7] | **Lars Glimelius**[8] | **Elias Coniavitis**[8] | **Thomas Held**[4,5,9] | **Thomas Haberer**[4] | **Amir Abdollahi**[1,2,3] | **Jürgen Debus**[2,3,4,5,9] | **Ivana Dokic**[1,2,3] | **Andrea Mairani**[1,4,7,9]

[1]Clinical Cooperation Unit Translational Radiation Oncology, German Cancer Consortium (DKTK) Core-Center Heidelberg, National Center for Tumor Diseases (NCT), Heidelberg University Hospital (UKHD) and German Cancer Research Center (DKFZ), Heidelberg, Germany

[2]Division of Molecular and Translational Radiation Oncology, Heidelberg Faculty of Medicine (MFHD) and Heidelberg University Hospital (UKHD), Heidelberg Ion-Beam Therapy Center (HIT), Heidelberg, Germany

[3]Heidelberg Institute of Radiation Oncology (HIRO), National Center for Radiation Oncology (NCRO), Heidelberg University and German Cancer Research Center (DKFZ) Heidelberg, Heidelberg, Germany

[4]Heidelberg Ion-Beam Therapy Center (HIT), Heidelberg University Hospital, Heidelberg, Germany

[5]Clinical Cooperation Unit Radiation Oncology, German Cancer Consortium (DKTK) Core-Center Heidelberg, National Center for Tumor Diseases (NCT), Heidelberg University Hospital (UKHD) and German Cancer Research Center (DKFZ), Heidelberg, Germany

[6]Department of Radiation Oncology, University of Pennsylvania, Philadelphia, Pennsylvania, USA

[7]National Center for Oncological Hadrontherapy (CNAO), Medical Physics, Pavia, Italy

[8]RaySearch Laboratories AB, Stockholm, Sweden

[9]Department of Radiation Oncology, Heidelberg University Hospital, Heidelberg Institute of Radiation Oncology (HIRO), National Center for Tumor Diseases (NCT), University Hospital Heidelberg, University Hospital Heidelberg, Heidelberg, Germany

Correspondence
Andrea Mairani, Heidelberg Ion-beam Therapy Center (HIT), Im Neuenheimer Feld 450, Heidelberg 69120, Germany.
Email: Andrea.Mairani@med.uni-heidelberg.de

Funding information
German Research Council, Grant/Award Number: SFB1389/2C05; National Center for Tumor Diseases, Grant/Award Numbers: 1030000042, 1030000043

Abstract

Background: Interpatient variation of tumor radiosensitivity is rarely considered during the treatment planning process despite its known significance for the therapeutic outcome.

Purpose: To apply our mechanistic biophysical model to investigate the biological robustness of carbon ion radiotherapy (CIRT) against DNA damage repair interference (DDRi) associated patient-to-patient variability in radiosensitivity and its potential clinical advantages against conventional radiotherapy approaches.

Methods and Materials: The "UNIfied and VERSatile bio response Engine" (UNIVERSE) was extended by carbon ions and its predictions were compared to a panel of in vitro and in vivo data including various endpoints and DDRi settings within clinically relevant dose and linear energy transfer (LET) ranges. The implications of UNIVERSE predictions were then assessed in a clinical patient scenario considering DDRi variance.

Results: UNIVERSE tests well against the applied benchmarks. While in vitro survival curves were predicted with an $R^2 > 0.92$, deviations from in vivo RBE data were less than 5.6% The conducted paradigmatic patient plan study

implies a markedly reduced significance of DDRi based radiosensitivity variability in CIRT (13% change of D_{50} in target) compared to conventional radiotherapy (62%) and that boosting the LET within the target further amplifies this robustness of CIRT (8%). In the case of heightened tumor radiosensitivity, a dose de-escalation strategy for photons allows a reduction of the maximum effective dose within the normal tissue (NT) from a D_2 of 2.65 to 1.64 Gy, which lies below the level found for CIRT (D_2 = 2.41 Gy) for the analyzed plan and parameters. However, even after de-escalation, the integral effective dose in the NT is found to be substantially higher for conventional radiotherapy in comparison to CIRT (D_{mean} of 0.75, 0.46, and 0.24 Gy for the conventional plan, its de-escalation and CIRT, respectively).

Conclusions: The framework offers adequate predictions of in vitro and in vivo radiation effects of CIRT while allowing the consideration of DRRi based solely on parameters derived from photon data. The results of the patient planning study underline the potential of CIRT to minimize important sources of interpatient divergence in therapy outcome, especially when combined with techniques that allow to maximize the LET within the tumor. Despite the potential of de-escalation strategies for conventional radiotherapy to reduce the maximum effective dose in the NT, CIRT appears to remain a more favorable option due to its ability to reduce the integral effective dose within the NT.

KEYWORDS
DNA damage repair interference, LET boost, UNIVERSE biophysical modelling

1 | INTRODUCTION

Despite the well-known existence of interpatient variance in tumor radiosensitivity, dose prescription in modern radiotherapy continues to follow a "one-size-fits-all" approach. This issue has motivated an ever-increasing effort to develop predictive biomarkers of radiosensitivity to allow patient stratification and individual dosing. However, up to date none has reached routine clinical use.[1,2] Besides the improved physical dose conformity and potentially increased biological effectiveness relative to conventional radiotherapy, high *linear energy transfer* (LET) carbon ion radiotherapy (CIRT) offers the ability to overcome key mechanisms known to cause radiation resistance.[3] Using different sublines of a syngeneic rat prostate tumor, Glowa et al. showed that consequently biological differences between tumors had a reduced effect on treatment outcome for carbon ion beams in comparison to conventional photon radiation.[4]

While several factors are considered to contribute to the intertumoral variability in radiation response, including hypoxia, cancer stem cell dynamics, and immune response,[1] the status of DNA damage repair (DDR) can be a decisive factor in many cases. For example, low expression levels of DDR proteins in localized prostate cancer[5,6] as well as somatic mutations of DDR genes in breast tumors[7] have been correlated to improved treatment response. Moreover, for HNSCC (head and neck squamous cell carcinoma) the heightened radiosensitivity of HPV-positive (human Papillomavirus) tumors is thought to be caused by a strong down regulation of several DDR enzymes.[8,9] And a somatic loss-of-function mutation of an important DNA damage detector (ATM) has been linked to favorable therapy outcome throughout numerous cancer types.[10] It is thus unsurprising that the expression and accumulation of DDR proteins have also gained increasing attention as potential prognostic biomarkers of radiosensitivity.[1,2,11]

In this work, we first present the extension of the "UNIfied and VERSatile bio response Engine" (UNIVERSE), a multipurpose mechanistic modeling framework of biological radiation effect,[12–16] to carbon ions and its benchmarks against in vitro and in vivo data. Other biophysical models of ion beam effect have already established themselves in clinical practice, such as the first version of the local effect model (LEM I)[17] applied in centers in Europe and parts of Asia (i.e., China) or the modified microdosimetric kinetic model (mMKM) used in Japanese centers.[18] In a previous study, the mMKM was found to outperform both LEM I and LEM IV in a panel of benchmarks including in vitro and in vivo measurements.[19] It is thus being considered to soon become the primary model for treatment planning at our facility. For these reasons and to maintain brevity, the performance of our model is compared to that of the mMKM. However, UNIVERSE offers the unique ability to model the effect of DDR interference (DDRi) using a single, dose- and LET-independent, parameter: The *radio sensitization factor* (RSF). The viability of this concept was shown in previous publications for sparsely ionizing radiation[12] as well as proton and helium beams.[15] To

our best knowledge, two other models have attempted to explicitly incorporate the effect of DDRi. However, one is purely empirical[20] and both are yet to be shown to provide accurate predictions in clinically relevant multi-energy fields.[21] Here, after validating the applicability of the RSF for carbon ions in different (clinically relevant) scenarios, we utilize UNIVERSE predictions in a patient planning study. There we assess, for the first time, the robustness against interpatient DDR-status variability in CIRT as opposed to conventional radiotherapy based on the change in the effective dose to the target and consider possible dose de-escalation strategies. Ultimately, the potential benefit of patient plans with a maximized LET within the target ("LET boost") is assessed. While this has been a long-suggested approach to overcome hypoxia induced radioresistence,[22] here, it is evaluated for the first time as a possible strategy to suppress DDR-driven heterogeneity of radiosensitivity.

2 | MATERIALS AND METHODS

2.1 | UNIVERSE

UNIVERSE is a mechanistic modeling framework which has been constantly developed and extended to enable the description and prediction of radiation action in biological systems while considering an increasing number of radiobiologically relevant parameters such as the applied dose rate and radiation quality or the presence of oxygen and radical scavengers within the system.[12–16] This study mainly extends upon the model of DDRi introduced and benchmarked for sparsely ionizing radiation and lighter ions (protons and helium ions) in earlier publications.[12,15] Here, core concepts are recalled, while the reader is kindly referred to the publications dedicated to these sub-modules of UNIVERSE for further details.

In general, the biological effect of radiation in UNIVERSE is derived from the clustering of DNA double strand breaks (DSB) within microscopic sub-domains of the nucleus. These domains may be thought of as representations of so-called giant-loops within chromatin which contain 1–3 Mbp of DNA[23–26] and an accumulation of DSB within them has been correlated to hampered DDR and increased probability of cell death.[27–29] Domains in which exactly 1 DSB was induced are called isolated DSB (iDSB) and those containing 2 or more DSB are named complex DSB (cDSB). This classification is shared with some related models.[30,31] Associating each isolated and complex DSB with a probability (K_{iDSB}, K_{cDSB}) of triggering cell death, the probability of the cell surviving the damage (S) can be written as[12,30]:

$$S = (1 - K_{iDSB})^{N_{iDSB}} \cdot (1 - K_{cDSB})^{N_{cDSB}}, \quad (1)$$

where N_{iDSB} and N_{cDSB} describe the number of domains containing isolated and complex damages within a nucleus, respectively.

Based on the assumption that the minimal prospects of clustered DSB to be repaired would not substantially decrease any further under inhibition of DDR enzymes, UNIVERSE only modifies the lethality of isolated DSB to model the resulting increase in radiosensitivity of affected cells.[12,15,32] More precisely, the DDRi is parametrized by increasing K_{iDSB} by a *radiosensitization-factor* (*RSF*),[12,15] so that the cells survival probability (S_{RSF}) changes to:

$$S_{RSF} = (1 - RSF \cdot K_{iDSB})^{N_{iDSB}} \cdot (1 - K_{cDSB})^{N_{cDSB}}. \quad (2)$$

UNIVERSE assumes that the effect of the induced damage classes is independent of the applied radiation quality. More specifically this means that the parameters such as K_{iDSB}, K_{cDSB}, and *RSF* are kept constant for a given cell line or DDRi, irrespective of the radiation type or energy. For sparsely ionizing radiation it has been well established, that the number of DSB per nucleus and applied unit dose α_{DSB} can be seen as constant within the clinically applied range.[33] Regardless of the dose distribution throughout the nucleus, UNIVERSE assumes that on the microscopic level of a given domain, the expected amount of DSB $\langle N_{DSB} \rangle$ can be derived from the constant α_{DSB}, the locally applied dose D and the number of domains within the nucleus N_{dom}:

$$N_{DSB} = \frac{\alpha_{DSB} \cdot D}{N_{dom}} \quad (3)$$

To determine the survival fraction of a cell population after irradiation, UNIVERSE uses a Monte Carlo approach which proceeds as follows: First, for at least 10^4 iterations, the microscopic dose distribution throughout the nucleus is simulated. This microscopic dose distribution determines the expected amount of DSB within the individual domains (Equation 3). Based on this expectancy value, the number of DSB for each domain is sampled following a Poisson distribution. Subsequently, the number of isolated and complex DSB (N_{iDSB} and N_{cDSB}) can be determined for each iteration, resulting in a survival probability S based on Equations 1 (or 2 if an RSF shall be applied). Ultimately, the survival fraction of the population is given by the mean value of S over all iterations.

The simulations for sparsely ionizing radiation (e.g., photons) and densely ionizing radiation (e.g., ion beams) only differ in the calculation of the microscopic dose distribution during the first step: For sparsely ionizing radiation one can assume a homogeneous distribution throughout the nucleus, so that the expected number of DSB within each domain can be given by Equation 3 while inserting the applied macroscopic dose.

However, in the case of ion fields, their heterogenous dose distribution on the microscopic scales requires a more detailed consideration of the nucleus geometry and particle tracks. In the current version of UNIVERSE, the nucleus is approximated as a cylinder with radius R_{nuc} and a volume of V_{nuc} containing cubic domains with side length d_{dom}. The particles are set to pass the nucleus parallel to its height-axis and the radial dose distribution (RDD) surrounding them is described with the Kiefer–Chatterjee parametrization.[34,35] The parametrization combines a "core" region with a constant dose D_c within the radius of r_{min} and an outer "penumbra" that reaches up to a radius of r_{max}, where the dose D_p decreases with increasing distance r (here in µm) from the track center[36,37]:

$$D_c = \frac{1}{\pi\, r_{min}^2}\left(\frac{LET}{\rho} - 2\,\pi\, K_p\, ln\left(\frac{r_{max}}{r_{min}}\right)\right), \quad (4)$$

$$D_p(r) = K_p\ r^{-2}, \quad (5)$$

$$K_p = 1.25 \cdot 10^{-4}\left(\frac{z^*}{\beta_{ion}}\right)^2, \quad (6)$$

where LET is the unrestricted linear energy transfer of the charged particle in keV/µm, ρ the density of water in g/cm^3, $\beta_{ion} = \frac{v}{c}$ (v: particle velocity, c: speed of light), and z^* the effective charge of the particle. The effective charge z^* is given by the Barkas formula[38]:

$$z^* = z_{ion}\left(1 - \exp\left(-125\ \beta_{ion}\ z_{ion}^{-2/3}\right)\right), \quad (7)$$

where z_{ion} is the charge of the fully ionized particle. The core radius is velocity dependent and is given by:

$$r_{min} = \beta_{ion} \cdot r_c, \quad (8)$$

with a constant r_c that was derived to be 11.6 nm.[34,37] The extent of the penumbra region (r_{max}) depends on the kinetic energy of the ion E_{kin} and was found to be approximated (in µm) by:

$$r_{max} = \gamma \cdot E_{kin}^{\delta}, \quad (9)$$

where E_{kin} is given in units of MeV/u as well as $\gamma = 0.062$ and $\delta = 1.7$.[35,37] The diffusion of DNA-damaging radicals created in the initial dose distribution is considered by a convolution of the RDD ($D(r)$) with a normal distribution kernel in which the standard deviation σ characterizes the diffusion length. The resulting RDD ($\tilde{D}(r)$) can be expressed as[39,40]:

$$\tilde{D}(r) = \int_0^{\infty} dr' r' \int_0^{2\pi} d\phi' D(r')\, f(r, r',\ \phi')$$

$$= \frac{e^{-r^2/2\sigma^2}}{\sigma^2} \int_0^{\infty} dr' r' e^{-\frac{r'^2}{2\sigma^2}}\ I_0\left(\frac{r\ r'}{\sigma^2}\right) D(r'), \quad (10)$$

with the modified Bessel function of order zero I_0. To facilitate the implementation of UNIVERSE on Graphics Processing Units (GPU), the resulting function was parametrized by a three-part piecewise function.[15] The area through which a tracks core needs to pass to deposit any dose within the nucleus can be computed based on the assumed radius of the nucleus and the maximum radius of the penumbra. The expected number of ions passing through this area can then be calculated using their LET and the applied dose. Based on this expectancy value, the number of considered tracks is sampled from a Poisson distribution for each iteration. They are then assigned to a random position within the previously calculated area. Ultimately, the microscopic dose distribution is considered to be the sum of RDDs surrounding these positions. However, the doses within an RDD can easily exceed several hundreds of Gy. At such high doses, single strand breaks (SSB) on opposite strands of the DNA start to accumulate and effectively represent DSB.[41–44] To consider this effect, a factor η is applied to the DSB yield in the step where the expected number of DSB within the individual domains is calculated (via Equation 3). The analytical expression for this factor was derived by Friedrich et al.[45] and depends on the yield of SSB per nucleus and applied unit dose (α_{SSB}), the length of the genome (L_{gen}) in base pairs (bp) and maximum interaction distance between two SSBs (t_{SSB}) in bp:

$$\eta = 1 + \frac{1 - e^{-\frac{\alpha_{SSB}\cdot D}{L_{gen}}\cdot t_{ssb}}}{3 - e^{-\frac{\alpha_{SSB}\cdot D}{L_{gen}}\cdot t_{ssb}}} \cdot e^{-\frac{\alpha_{DSB}\cdot D}{L_{gen}}\cdot t_{ssb}} \cdot \frac{\alpha_{SSB}}{\alpha_{DSB}}. \quad (11)$$

But, this expression results in a monotonic increase of the DSB yield with LET, while some Monte Carlo Simulations suggest a saturation above ~100 keV/µm for carbon ions.[46] To account for this effect the t_{SSB} parameter was kept at 3 bp for the previously published lighter ions (protons and helium ions[15]) and reduced to 2 bp for carbon ions. While this can be seen as a small discrepancy, in future developments, alternative descriptions of the DSB yield may be considered to improve mechanistic consistency.

With the exception of t_{SSB} described above the set of parameters ($\alpha_{DSB}, \alpha_{SSB}, \sigma, d_{dom}, L_{gen}, R_{nuc}, V_{nuc}$) established in a previous publication were fully adopted with no changes for all calculations if not stated otherwise. Their values can be found in the Table S1.

3 | BENCHMARKS OF THE DEVELOPED MODEL

For each comparison of model predictions against measurements from the literature, the biological parameters (K_{iDSB}, K_{cDSB}, and RSF) were derived solely from data obtained after photon irradiation of the

same biological endpoint as reported by the corresponding source. These parameters are then used for carbon ion predictions without any further modification. For the benchmarks against the carbon ion irradiation data by Furusawa et al.[47] and Saager et al.[48] the K_{iDSB} and K_{cDSB} were already obtained in previous publications.[15,16] In the case of the remaining predictions presented in this study, both the photon and carbon ion irradiation data were obtained from Suzuki et al,[49] Flint et al.,[20] Cartwright et al.,[50] and Lerch et al.[51] Following the procedure detailed in a previous publication,[12] the K_{iDSB} and K_{cDSB} values are derived by fitting the model for sparsely ionizing radiation and Equation 1 to the photon data using the *curve_fit* routine of the *scipy* library for *Python*. For cell lines that are reportedly subject to DDRi (e.g., DNA-PK deficient mutants), these two parameters are set to those derived for the wild type (e.g., DNA-PK proficient parent) of the cell line and Equation 2 is fitted to determine the *RSF*.

When cell survival after irradiation with^{12C} was computed for reported LET values we assumed the (quasi) in-track-segment condition (fixed LET) to be satisfied within the nuclei. However, LET values taken from literature are associated with an intrinsic uncertainty as they are not always calculated via the same definition.[52] When available the dose-averaged LET was chosen.

For mixed radiation fields, such as spread-out Bragg-peaks (SOBP), endpoint-specific sets of linear-quadratic model (LQM) parameters were established as a function of LET for primary C ions and secondary fragments by fitting the LQM to survival predicted by UNIVERSE. On their basis, Monte Carlo codes determined the biological effect of the mixed radiation field and relative biological effectiveness (RBE) as detailed in a previous publication[53] and in the Supplementary Material.

4 | PATIENT PLANS

The treatment plans for an adenoid cystic carcinoma case (planning target volume (PTV) 275 cm^3) was optimized with the clinical version RayStation11B (RaySearch Laboratories, Stockholm, Sweden) for photons. The standard intensity modulated particle therapy (IMPT) plan using carbon ions was optimized utilizing a research version of RayStation11B, with support for RBE optimization with LQM parameters as described in the supplementary Material. The standard CIRT plan was optimized for the isocentric gantry, following institutional guidelines, using three beams with angulation from 40° to 90°. For the LET boosted plan, 7 beams of different angles, from 310° to 130°, were applied to allow an enhanced LET throughout the gross tumor volume (GTV) while maintaining a uniform biological dose within the target. The LET boost was enabled by pre-optimizing the plan in RayStation 2023B and finalizing the optimization in the research version Raystation 11B. In this study, the Normal tissue is defined as the body region without the PTV, cropped in infero-superior considering an extension of 2 cm of the target. Its α/β ratio was set to 2 Gy ($\alpha_x = 0.05\ Gy^{-1}$, $\beta_x = 0.025\ Gy^{-2}$), a standard choice for NT. The underlying intertumoral heterogeneity in DDR was chosen to be reflected by the HPV status due to its role in HNSCC. The modeling parameters of the target were set to the values obtained from the in vitro data set by Lerch et al.

5 | RESULTS

5.1 | Survival after ^{12}C irradiation over clinical dose and LET range

In Figure 1a, predicted survival of HSG (left panel) and V79 (right panel) cells after irradiation with ^{12}C ion beams over a wide LET range are compared to measured values from Furusawa et al.[47] The cell line dependent parameters (K_{iDSB}, K_{cDSB}) were already derived in a previous publication[15] based on the photon data reported by Furusawa et al.[47] and are given in Table 1. For UNIVERSE, the mean relative difference between the measured and predicted logarithm of survival fraction (MRDLS) were 13.4% and −16.7% for HSG and V79, respectively. As a comparison, predictions of the mMKM were calculated following the procedure detailed in a previous publication.[19] The mMKM scored an MRDLS of 16.6% and −13.7% for HSG and V79, respectively.

Figure 1b depicts measured cell survival as a function of dose for 15 cell lines irradiated with photons and ^{12}C ion beams at 13 and 77 keV/μm taken from Suzuki et al.[49] with respective simulations by UNIVERSE (lines). In the last panel, the percentage difference between experimental and UNIVERSE-derived D_{10} (i.e., the dose required to reach a survival fraction of 10%), ΔD_{10}, for 13 and 77 keV/μ m is summarized in terms of box plots. At 13 and 77 keV/μ m, ΔD_{10} mean ± standard deviation was 3.7% ± 8.2% and 21.2% ± 21.9%, respectively. The parameters K_{iDSB} and K_{cDSB} were derived from the photon data and are reported in Table 1.

5.2 | Survival of DNA repair deficient and HPV-positive cell lines after carbon ion irradiation

Figure 2a shows the predictions for survival data of M059K cells and their DNA-PK deficient mutant (M059J) after irradiation with photons and ^{12}C ions at 13.5, 27.9, and 60.5 keV/μm obtained by Flint et al.[20] The cell line dependent parameters K_{iDSB} and K_{cDSB} as well as the RSF were derived from photon survival curves and are given in Table 1. The R^2 values (coefficient of

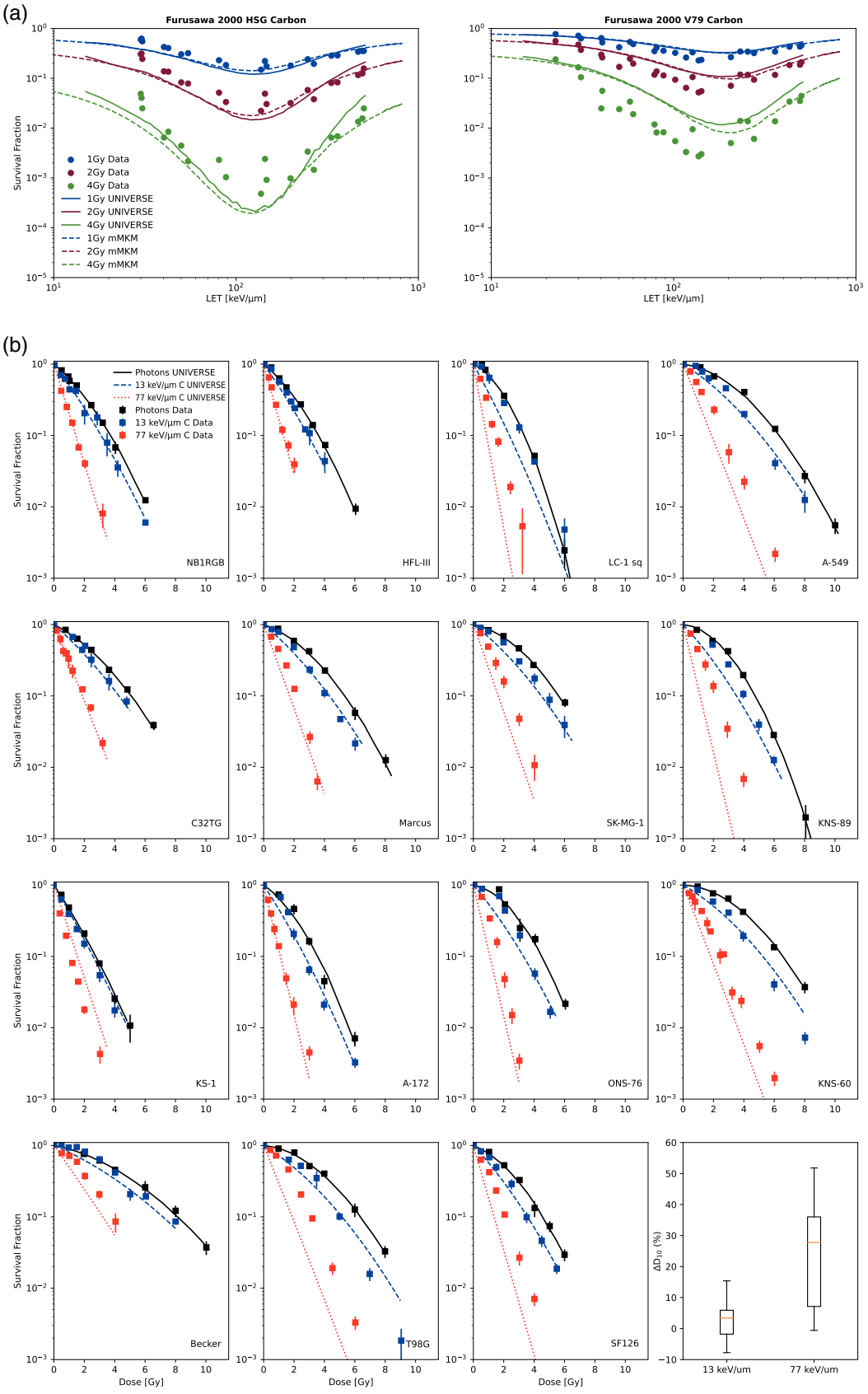

FIGURE 1 (a) Survival of HSG (left panel) and V79 (right panel) cells after irradiation with ^{12}C ion beams at clinically relevant dose and linear energy transfer (LET) values from Furusawa et al.,[47] with respective simulations by UNIVERSE and the modified Microdosimetric Kinetic Model (mMKM). (b) Survival fraction of different cell lines (squares with error bars) after irradiation with photons and ^{12}C ion beams at 13 and 77 keV/µm from Suzuki et al.[49] with respective simulations by UNIVERSE (lines). In the last panel the percentage difference between experimental and UNIVERSE-derived D_{10} for 13 and 77 keV/μ m is summarized in terms of box plots.

TABLE 1 Numerical values of the parameters of UNIVERSE derived for all benchmarks.

Cell line/biological endpoint	K_{iDSB}	K_{cDSB}	RSF
HSG[47]	8.18E-3 ± 0.64E-3	0.38 ± 0.015	–
V79[47]	4.85E-3 ± 0.20E-3	0.13 ± 0.0035	–
NB1RGB[49]	1.19E-2 ± 0.013E-2	0.32 ± 0.0029	–
HFL-III[49]	1.14E-2 ± 0.014E-2	0.38 ± 0.0030	–
LC-1 sq[49]	6.49E-3 ± 0.57E-3	0.73 ± 0.011	–
A549[49]	1.80E-3 ± 0.073E-3	0.27 ± 0.0016	–
C32TG[49]	6.96E-3 ± 0.072E-3	0.24 ± 0.0016	–
Marcus[49]	4.81E-3 ± 0.087E-3	0.28 ± 0.0018	–
SK-MG-1[49]	2.56E-3 ± 0.14E-3	0.31 ± 0.0030	–
KNS-89[49]	6.47E-4 ± 5.28E-4	0.53 ± 0.011	–
KS-1[49]	2.13E-2 ± 0.0087E-2	0.24 ± 0.0019	–
A-172[49]	9.90E-3 ± 0.21E-3	0.48 ± 0.0045	–
ONS-76[49]	2.03E-3 ± 0.29E-3	0.53 ± 0.0064	–
KNS-60[49]	4.58E-4 ± 0.79E-4	0.28 ± 0.0017	–
Becker[49]	2.72E-3 ± 0.029E-3	0.13 ± 0.00063	–
T98G[49]	1.38E-3 ± 0.091E-3	0.27 ± 0.0020	–
SF126[49]	5.51E-3 ± 0.10E-3	0.38 ± 0.0022	–
M059K[20]	1.06E-2 ± 0.0078E-2	0.14 ± 0.0055	–
M059J[20]	Set equal to M059K	Set equal to M059K	5.41 ± 0.27
CHO WT[50]	4.38E-3 ± 1.37E-3	0.23 ± 0.027	–
V3[50]	Set equal to CHO WT	Set equal to CHO WT	9.60 ± 0.19
Xrs5[50]	Set equal to CHO WT	Set equal to CHO WT	14.85 ± 0.50
UMM-SCC-6 (HPV-neg)[51]	1.18E-3 ± 0.79E-3	0.45 ± 0.031	–
UPI:SCC154 (HPV-pos)[51]	Set equal to HPV-neg	Set equal to HPV-neg	10.44 ± 0.80
Rat Spinal Cord[48]	6.5E-5 ± 1.77E-5	8.5E-3 ± 0.39E-3	–

determination) for fits of the photon data show a mean of 0.99, while predictions for ^{12}C ions reach a mean of 0.92. In Figure 2b UNIVERSE predictions for CHO cells and their two NHEJ response-deficient mutant cell lines (V3 being DNA-PKcs-deficient and xrs-5 being Ku80-deficient) after irradiation with photons (left panel) and ^{12}C ions at 13 keV/µm (central panel) and mid-SOBP (50 keV/µm, right panel) are compared against experimental data taken from Cartwright et al.[50] Again, the K_{iDSB}, K_{cDSB}, and RSF values were obtained based on the photon data and are reported in Table 1. The R^2 values for fits of the photon data achieved a mean of 1.00, while predictions for ^{12}C ions reach a mean of 0.96.

In the upper-left panel of Figure 3 cell survival data (empty squares with error bars) of HPV-negative cells (UMM-SCC-6) and HPV-positive cells (UPI:SCC154) after irradiation with photons (upper left panel) and carbon ions (upper right panel) obtained from Lerch et al.[51] are shown. The respective UNIVERSE predictions are depicted as lines. The values for the parameters K_{iDSB}, K_{cDSB}, and RSF were derived from the photon data in the upper-left panel and are given in Table 1. The R^2 values for fits of the photon data achieved a mean of 0.99, while predictions for ^{12}C ions reach a mean of 0.98. In the lower panels of Figure 3, survival fractions of five HPV-positive and five HPV-negative cells irradiated with 6 Gy photons (left) or 3 Gy carbon ions (right) are shown together with UNIVERSE prediction for UMM-SCC-6 and UPI:SCC154 cells as representatives for HPV-negative and positive cell lines, respectively.

5.3 | In vivo RBE after carbon ion irradiation

In Figure 4, the in vivo RBE in rat spinal cord (RSC) measured by Saager et al.[48] are compared against UNIVERSE simulations. The original study determined the RBE based on the TD50-values (dose at 50% effect probability) for the clinical endpoint of paresis grade II that was detected within 300 days. The RSC was positioned at six depths within a carbon ion SOBP with one (1Fx), two (2 Fx), or six (6 Fx) fractions applied. The values for K_{iDSB} and K_{cDSB} were obtained in an earlier publication[16] and are reported in Table 1. The mean absolute deviations (MAD: the absolute value of the percentage difference between measured and predicted RBE averaged over the values for 1Fx, 2Fx

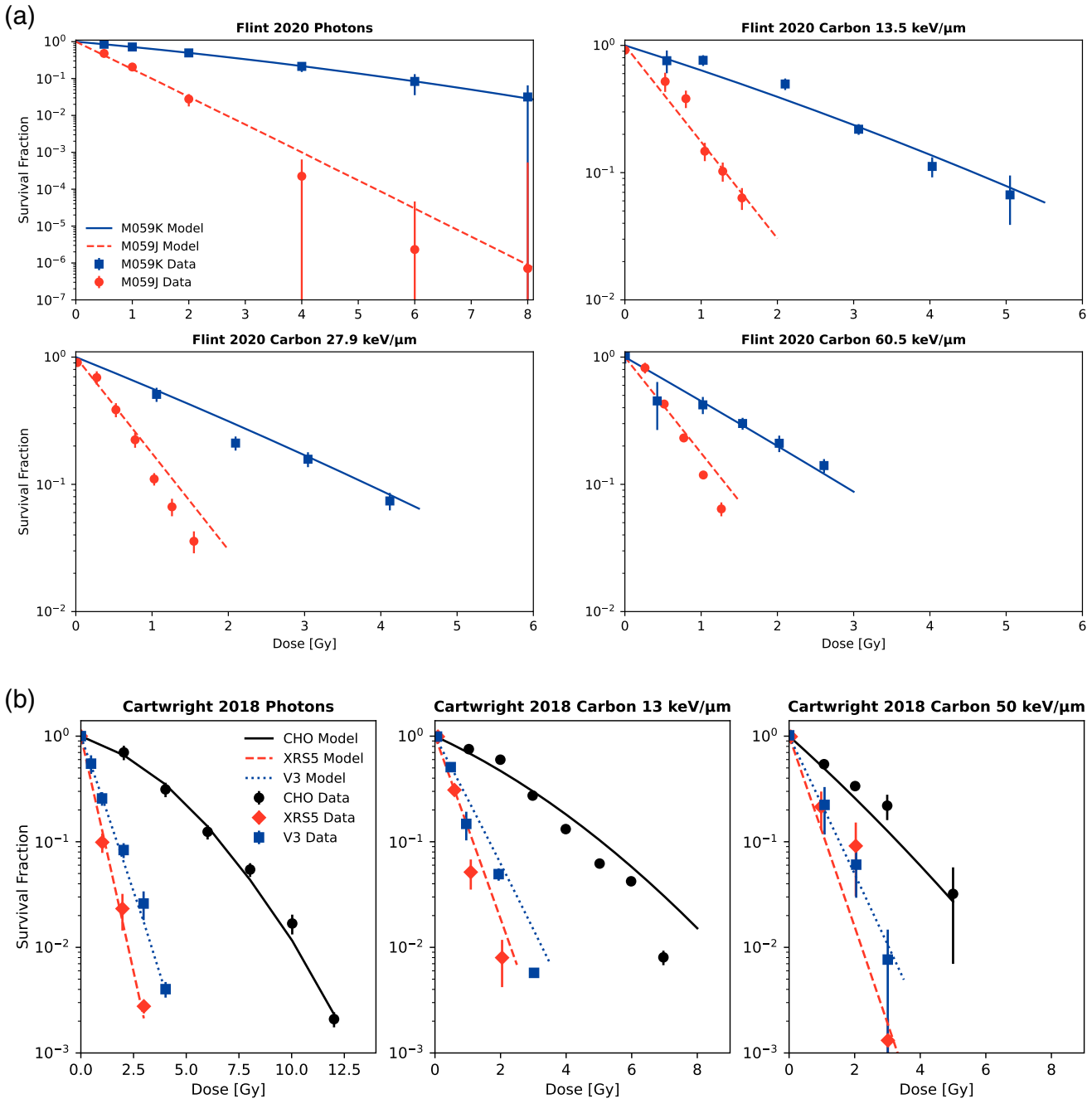

FIGURE 2 (a) Survival data of M059K cells and their DNA-dependent protein kinase (DNA-PK)-deficient mutant (M059J) after irradiation with photons and ^{12}C ions at 13.5, 27.9, and 60.5 keV/µm from Flint et al.[20] and respective simulations by UNIVERSE. (b) Survival data of CHO cells and their two NHEJ response-deficient mutants (V3 cell line is DNA-PKcs-deficient and xrs-5 cell line is Ku80-deficient) after irradiation with photons (left panel) and ^{12}C ions at 13 and 50 keV/µm (center and left panels) from Cartwright et al.[50] and respective simulations by UNIVERSE.

and 6Fx) were found to be 5.29%, 2.54%, 5.56% for 1 Fx, 2 Fx and 6 Fx, respectively.

5.4 | Obtained endpoint dependent model parameters

The numerical values of the endpoint dependent model parameters which were obtained for the presented benchmarks based on photon irradiation data are summarized in Table 1.

5.5 | Patient planning study

Figure 5a–c shows the effective dose distributions of irradiation plans for conventional photon radiotherapy, CIRT, and CIRT with an increased target LET,

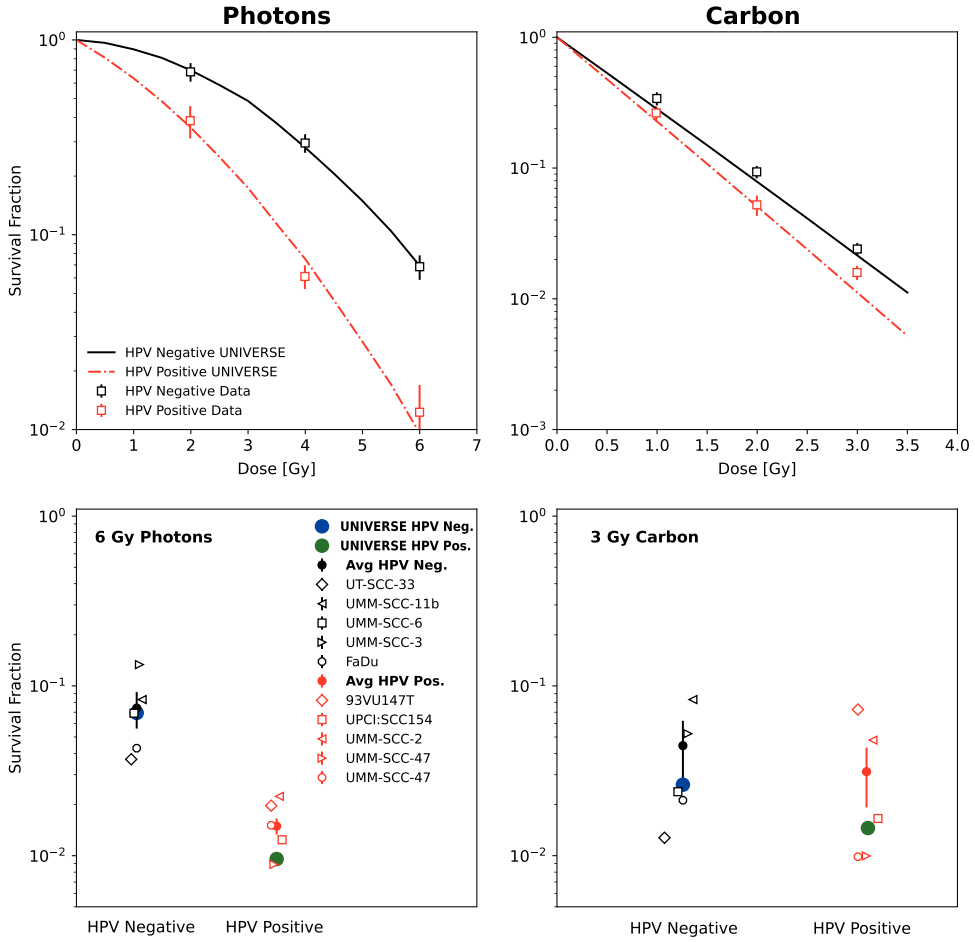

FIGURE 3 Survival data (empty squares with error bars) of UMM-SCC-6 cells (HPV-negative) and UPI:SCC154 cells (HPV-positive) after irradiation with photons (upper left panel) and carbon ions (upper right panel). The respective UNIVERSE predictions are depicted as lines. Survival data of five HPV-negative cells and HPV-positive cells after 6 Gy photon irradiation are shown in the lower left panel. Survival data of five HPV-negative cells and HPV-positive cells after 3 Gy carbon ion irradiation are shown in the lower right panel. All data taken from Lerch et al.[51] The UNIVERSE predictions are based on UMM-SCC-6 and UPI:SCC154 cells.

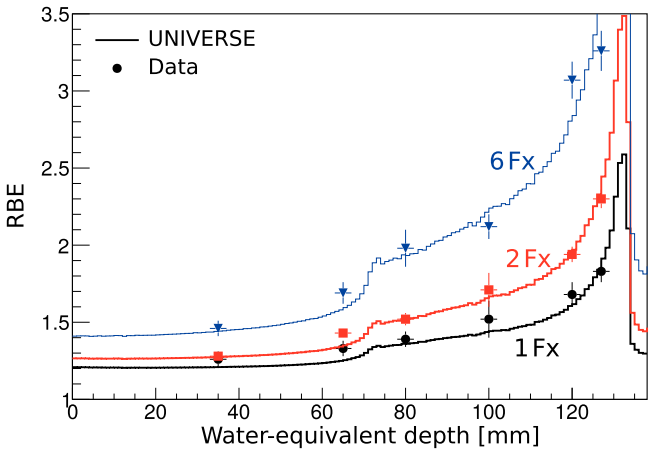

FIGURE 4 Measured (points with error bars, Saager et al.[48]) and predicted (lines) RBE in RSC irradiated at 6 positions within a clinical SOBP using one (1 Fx), two (2 Fx) or six (6 Fx) carbon ion fractions. The RBE is calculated based on the TD50-values (dose at 50% effect probability) for the clinical endpoint of paresis grade II that was detected within 300 days.

respectively, for a patient with a head and neck tumor. The plans were optimized to induce the same effect as a 3 Gy photon irradiation in HPV-negative (UMM-SCC-6) cells within the clinical target volume (CTV), based on the parameters established above (Table 1 and Figure 3). From the LET-volume-histogram (LVH) in Figure 5d one can derive that the LET that is at least received by 50% of the GTV (LET_{50}) was about 58.1 keV/µm for the standard CIRT plan and 100.8 keV/µm for the CIRT plan with an LET boost. For each plan the effective dose-volume-histogram (DVH) within the GTV is shown in Figure 5e, assuming the parameters derived for HPV-negative (UMM-SCC-6) and HPV-positive (UPI:SCC154) cells established prior (Table 1 and Figure 3). The effective dose represents the physical photon dose needed to achieve the observed effect in HPV-negative (UMM-SCC-6) cells. The effective dose that is at least received by 50% of the GTV (D_{50}) was found to be 3 and 4.86 Gy in the photon plan, 3 and 3.38 Gy in the CIRT plan, and 2.96 and 3.21 Gy in

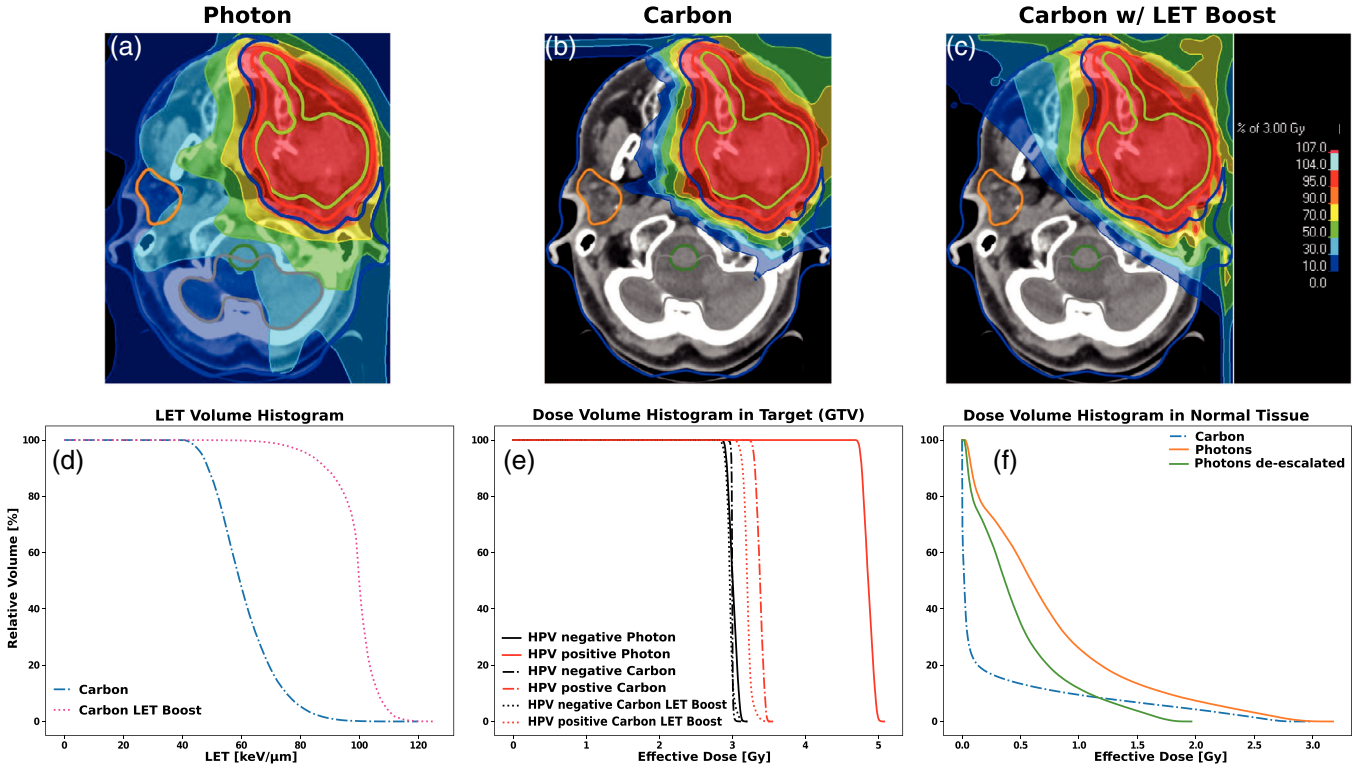

FIGURE 5 (a) Photon, (b) carbon ion radiotherapy (CIRT), and (c) CIRT with LET boost plans for a head and neck tumor patient optimized to induce the effect of 3 Gy in HPV-negative (UMM-SCC-6) cells (Table 1 and Figure 3) within the target (GTV). (d) LET-volume-histogram (LVH) of the CIRT and CIRT with LET boost plan within the GTV. (e) Effective dose-volume-histogram (DVH) within the GTV for all plans assuming the parameters derived for HPV-negative (UMM-SCC-6) and HPV-positive (UPI:SCC154) cells established prior (Table 1 and Figure 3). The effective dose represents the physical photon dose needed to achieve the observed effect in HPV-negative (UMM-SCC-6) cells. (f) DVH within the normal tissue (NT) for the photon and CIRT plans. The effective dose represents the physical photon dose needed to achieve the observed effect at an α/β ratio of 2 Gy, a standard choice for NT. In addition, a DVH is shown for the case that the prescribed dose for photons is de-escalated for an HPV-positive case to match the effect in an HPV-negative tumor.

the CIRT plan with the LET boost, for the HPV-negative and HPV-positive case, respectively. For the presented case, the change in DNA repair proficiency connected to the HPV status is thus predicted to have a reduced impact for both the standard (+13% effective dose) and LET enhanced (+8%) CIRT plan in comparison to the conventional photon plan (+62%). The DVH within the normal tissue (NT) for the photon and CIRT plans are shown in Figure 5f. In this case, the effective dose represents the physical photon dose needed to achieve the observed effect at an α/β ratio of 2 Gy ($\alpha_x = 0.05$ Gy^{-1}, $\beta_x = 0.025$ Gy^{-2}), a standard choice for NT. In addition, a DVH is shown for the case that the prescribed dose for photons is de-escalated for an HPV-positive case to match the effect in an HPV-negative tumor. In the presented setting, the de-escalation results in a considerable reduction of the maximum effective dose, with the D_2 (minimum effective dose within the 2% volume receiving the highest effective dose) falling from 2.65 Gy to 1.64 Gy, which lies below the level found for CIRT ($D_2 = 2.41$ Gy). At the same time, the integral effective dose to the NT remains notably higher in comparison to CIRT, as the average effective dose (D_{mean}) is found to drop from 0.75 to 0.46 Gy after de-escalation, while for CIRT it lies at 0.24 Gy.

6 | DISCUSSION

Based on only two variables (K_{iDSB} and K_{cDSB}) derived solely from photon data, the carbon model of UNIVERSE was shown to predict in vitro cell survival for numerous cell lines and LET settings (Figure 1) as well as the RBE of an in vivo endpoint within an SOBP (Figure 4) with appropriate accuracy. Considering the benchmarks in Figure 1, UNIVERSE was found to perform comparably to the mMKM. While it slightly outperformed it on the HSG data by Furusawa et al., the opposite was found for the V79 data (Figure 1a). When the percentage difference between the predicted D_{10} and the measurements compiled by Suzuki et al. (Figure 1b) was calculated for the mMKM (cp. Figure S1), values of 9.7% ± 7.8% and 23.3% ± 19.7% were found for 13 and 77 keV/μ m, respectively, indicating a slightly better performance by UNIVERSE (3.7% ± 8.2% and 21.2% ± 21.9%) for that dataset.

While the performance of the basic carbon model is favorable, the greatest value of our framework may lie in its unique ability to account for DDRi through a single, dose- and LET-independent, parameter. The applicability of this RSF parameter to carbon ions was demonstrated for several beam energies and cell lines based on literature data (Figures 2 and 3). In an earlier study regarding protons and helium ions,[15] UNIVERSE was shown to correctly predict certain trends including a decrease of the impact of DDRi on cell survival with increasing LET or a diminishment of RBE in cells affected by DDRi. In this study, these tendencies appear to be confirmed for carbon ions, too: Based on the D_{10} values reported by Flint et al. (Figure 2a)[20] the *sensitivity enhancement ratio*, or SER_{10}, (ratio between the dose applied to reference cells and the dose applied to DDRi affected cells to reach iso-effect, here: 10% survival) between M059K and M059J was found to be 3.95 for photons. For carbon ions it declined to 3.36, 3.22, and 2.9 at 13.5, 27.9, and 60.5 keV/µm, respectively. Furthermore, while the RBE in M059K increased from 1.33 over 1.52 to 1.80 for the same carbon LETs, it increased with a smaller slope and values for M059J cells who exhibited RBEs of 1.13, 1.25, and 1.33 over the same range. Although numerical values of D_{10} where not reported by Cartwright et al. (Figure 2b), the same trends can be inferred from the survival curves where the D_{10} values for the DDRi cell lines (xrs5 and V3) virtually do not change as the LET is increased, while for the CHO WT the values visibly decrease.

The reduced impact of DDRi in high LET carbon beams can be seen particularly well in Figure 3: For HPV-positive (DDRi) cell lines a dose of 3 and 6 Gy where necessary for carbon ions and photons, respectively, to reach a survival of slightly above 1%. When switching to HPV-negative cells the same doses lead to a considerably increased cell survival for photons, while it hardly changed for the carbon beam. By accurately predicting the survival curves of these data sets, UNIVERSE demonstrated its capability to capture these important trends also for carbon ions.

In our model, the decreased sensitivity (or robustness) of CIRT against DDRi, especially at high LET, arises due to our assumption that it predominantly affects the lethality of isolated DSB (Equation 2). CIRT induces higher levels of complex DSB than sparsely ionizing radiation due to the high local doses within their tracks, which further increase with rising LET (Equations 4–6). Thus, the lethality of isolated DSB and the introduction of an RSF that reflects the DDRi, plays a diminishing role for the effectiveness of (high-LET) CIRT.

To investigate the clinical implications of the model, a representative treatment planning study was conducted based on a patient with a head and neck tumor (Figure 5), where the underlying intertumoral heterogeneity in DDR was chosen to be reflected by the HPV status. It shall be emphasized that this treatment plan analysis is to be seen as paradigmatic and the resulting values may vary for other treatment plans depending on many factors, including the model parameters, patient geometry and beam settings. Nonetheless, in the presented case, the impact of the DDRi on the D_{50} was substantially reduced from the photon plan to the standard CIRT plan (62% change in D_{50} to 13%). Standard CIRT may thus already offer a notably higher robustness against DDRi based intertumoral variance in radiosensitivity. The CIRT plan with enhanced LET reduced the effect of the DDRi even further, nearly halving it (13% change in D_{50} to 8%). Advanced treatment techniques such as multi-ion[54] or particle arc therapy[55] which provide improved high-LET coverage throughout the target may thus be especially suitable to minimize the uncertainty in treatment outcome.

Unsurprisingly, the exposure of the NT in CIRT was found to be considerably lower in comparison to the conventional photon plan. It may however be argued that, in cases in which the DDR status is known, the photon dose could be de-escalated. In the case of HPV-positive head and neck tumors, such an approach has indeed gained serious attention.[56] In our study we reduced the applied dose by the factor needed to match the effect in an HPV-positive tumor to that in an HPV-negative one to represent such an approach. While the maximum effective dose was reduced (from a D_2 of 2.65–1.64 Gy) below that of the CIRT plan (D_2 of 2.41), indicating a potential reduction of toxicity in ipsilateral organs, CIRT continues to apply less integral effective dose to the NT (D_{mean} of 0.75, 0.46, and 0.24 Gy for the conventional plan, its de-escalation and CIRT, respectively). CIRT may thus remain less toxic for organs far from the target and placed contralaterally as well as maintain reduced risk of secondary malignancy, especially in young patients. Furthermore, one needs to consider that in many cases the DDRi status remains undetermined and even if it is known large uncertainties remain regarding the exact amount of de-escalation that may be appropriate. Taken together, conventional photon therapy with dose de-escalation might only become a viable option over CIRT in cases where the maximum dose to specific organs is paramount and once reliable bio markers would allow to deduce the suitable dose reduction.

Unfortunately, the RSF cannot capture the effect of all mechanisms underlying interpatient variability in tumor radiosensitivity, most notably hypoxia. However, one of the strategies proposed to overcome hypoxia related radioresistance has been to maximize the LET within the target,[22] the same approach that our study demonstrated to suppress DDRi based heterogeneity in treatment outcome. This underlines the need to advance technologies and methods that may provide robust high-LET coverage of the tumor and the study of their clinical applicability, as they could hold the key to reducing some of the most important sources of patient-to-patient divergence in therapy outcome.

7 | CONCLUSION

UNIVERSE was successfully extended to include carbon ions, allowing the prediction of their biological effect even under interference with DDR within the target using not more than three variables derived from photon data. The conducted patient planning study implies that CIRT offers higher robustness against DDRi based interpatient variance in tumor radiosensitivity. It also appears to remain a more favorable option over conventional radiotherapy in most cases, even when the DDRi status is known, due to its ability to prevent low-dose exposure of large parts of the NT and persisting uncertainties connected to the appropriate extent of photon dose de-escalation. Boosting the LET within the target further decreased the dependence of the predicted biological effect on DDR proficiency, providing a possible avenue to maximize the clinical potential of CIRT in mitigating crucial uncertainties in radiotherapy.

ACKNOWLEDGMENTS

This work was supported by German Research Council (DFG-Unite: SFB1389/2C05) and intramural funds from National Center for Tumor Diseases (NCT-PRO: 1030000042 and Biodose: 1030000043 programs). The funders had no role in study design, data collection and analysis, decision to publish or preparation of the manuscript.

Open access funding enabled and organized by Projekt DEAL.

CONFLICT OF INTEREST STATEMENT

JD reports grants from CRI—The Clinical Research Institute GmbH grants from View Ray Inc., grants from Accuray International Sarl, grants from Accuray Incorporated, grants from RaySearch Laboratories AB, grants from Vision RT limited, grants from Merck Serono GmbH, grants from Astellas Pharma GmbH, grants from AstraZeneca GmbH, grants from Siemens Healthcare GmbH, grants from Merck KGaA, grants from Solution Akademie GmbH, grants from Ergomed PLC Surrey Research Park, grants from Siemens Healthcare GmbH, grants from Quintiles GmbH, grants from Pharmaceutical Research Associates GmbH, grants from Boehringer Ingelheim Pharma GmbH Co, grants from PTW-Freiburg Dr. Pychlau GmbH, grants from Nanobiotix AA, outside the submitted work. AA and report grants and other from Merck and EMD, grants and other from Fibrogen, other from BMS, other from BioMedX, other from Roche, outside the submitted work. LG and EC are employed by RaySearch Laboratories AB.

REFERENCES

1. Price JM, Prabhakaran A, West CML. Predicting tumour radiosensitivity to deliver precision radiotherapy. *Nat Rev Clin Oncol*. 2023;20(2):83-98. doi:10.1038/s41571-022-00709-y
2. Forker LJ, Choudhury A, Kiltie AE. Biomarkers of tumour radiosensitivity and predicting benefit from radiotherapy. *Clinical Oncology*. 2015;27(10):561-569. doi:10.1016/j.clon.2015.06.002
3. Durante M, Debus J, Loeffler JS. Physics and biomedical challenges of cancer therapy with accelerated heavy ions. *Nat Rev Phys*. 2021;3(12):777-790. doi:10.1038/s42254-021-00368-5
4. Glowa C, Karger CP, Brons S, et al. Carbon ion radiotherapy decreases the impact of tumor heterogeneity on radiation response in experimental prostate tumors. *Cancer Lett*. 2016;378(2):97-103. doi:10.1016/j.canlet.2016.05.013
5. Hasegawa T, Someya M, Hori M, et al. Expression of Ku70 predicts results of radiotherapy in prostate cancer. *Strahlenther Onkol*. 2017;193(1):29-37. doi:10.1007/s00066-016-1023-7
6. Bouchaert P, Guerif S, Debiais C, Irani J, Fromont G. DNA-PKcs expression predicts response to radiotherapy in prostate cancer. *Int J Radiat Oncol Biol Phys*. 2012;84(5):1179-1185. doi:10.1016/j.ijrobp.2012.02.014
7. Kim KH, Kim HS, seob KimS, et al. Increased radiosensitivity of solid tumors harboring *ATM* and *BRCA1/2* mutations. *Cancer Res Treat*. 2021;54(1):54-64. doi:10.4143/crt.2020.1247
8. Zhou C, Parsons JL. The radiobiology of HPV-positive and HPV-negative head and neck squamous cell carcinoma. *Expert Rev Mol Med*. 2020;22:e3. doi:10.1017/erm.2020.4
9. Arenz A, Ziemann F, Mayer C, et al. Increased radiosensitivity of HPV-positive head and neck cancer cell lines due to cell cycle dysregulation and induction of apoptosis. *Strahlenther Onkol*. 2014;190(9):839-846. doi:10.1007/s00066-014-0605-5
10. Pitter KL, Casey DL, Lu YC, et al. Pathogenic ATM mutations in cancer and a genetic basis for radiotherapeutic efficacy. *J Natl Cancer Inst*. 2021;113(3):266-273. doi:10.1093/jnci/djaa095
11. Willers H, Gheorghiu L, Liu Q, et al. DNA damage response assessments in human tumor samples provide functional biomarkers of radiosensitivity. *Semin Radiat Oncol*. 2015;25(4):237-250. doi:10.1016/j.semradonc.2015.05.007
12. Liew H, Klein C, Zenke FT, et al. Modeling the effect of hypoxia and DNA repair inhibition on cell survival after photon irradiation. *Int J Mol Sci*. 2019;20(23):6054. doi:10.3390/ijms20236054
13. Liew H, Mein S, Debus J, Dokic I, Mairani A. Modeling direct and indirect action on cell survival after photon irradiation under normoxia and hypoxia. *Int J Mol Sci*. 2020;21(10):3471. doi:10.3390/ijms21103471
14. Liew H, Mein S, Dokic I, et al. Deciphering time-dependent DNA damage complexity, repair, and oxygen tension: a mechanistic model for FLASH-dose-rate radiation therapy. *Int J Radiat Oncol Biol Phys*. 2021;110(2):574-586. doi:10.1016/j.ijrobp.2020.12.048
15. Liew H, Meister S, Mein S, et al. Combined DNA damage repair interference and ion beam therapy: development, benchmark, and clinical implications of a mechanistic biological model. *Int J Radiat Oncol Biol Phys*. 2022;112(3):802-817. doi:10.1016/j.ijrobp.2021.09.048
16. Liew H, Mein S, Tessonnier T, et al. Impact of DNA repair kinetics and dose rate on RBE predictions in the UNIVERSE. *Int J Mol Sci*. 2022;23(11):6268. doi:10.3390/ijms23116268
17. Scholz M, Kellerer AM, Kraft-Weyrather W, Kraft G. Computation of cell survival in heavy ion beams for therapy. *Radiat Environ Biophys*. 1997;36(1):59-66. doi:10.1007/s004110050055
18. Inaniwa T, Kanematsu N, Matsufuji N, et al. Reformulation of a clinical-dose system for carbon-ion radiotherapy treatment planning at the National Institute of Radiological Sciences, Japan. *Phys Med Biol*. 2015;60(8):3271. doi:10.1088/0031-9155/60/8/3271
19. Mein S, Klein C, Kopp B, et al. Assessment of RBE-weighted dose models for carbon ion therapy toward modernization of clinical practice at HIT: in vitro, in vivo, and in patients. *Int J Radiat Oncol Biol Phys*. 2020;108(3):779-791. doi:10.1016/j.ijrobp.2020.05.041
20. Flint DB, Bright SJ, McFadden CH, et al. An empirical model to predict survival curve and relative biological effectiveness after helium and carbon ion irradiation based solely on the cell survival

after photon irradiation. *bioRxiv*. Published online June 20, 2020. doi:10.1101/2020.06.19.161836
21. McMahon SJ, McNamara AL, Schuemann J, Paganetti H, Prise KM. A general mechanistic model enables predictions of the biological effectiveness of different qualities of radiation. *Sci Rep*. 2017;7(1):10790. doi:10.1038/s41598-017-10820-1
22. Bassler N, Jäkel O, Søndergaard CS, Petersen JB. Dose- and LET-painting with particle therapy. *Acta Oncol*. 2010;49(7):1170-1176. doi:10.3109/0284186X.2010.510640
23. Sachs RK, van den Engh G, Trask B, Yokota H, Hearst JE. A random-walk/giant-loop model for interphase chromosomes. *Proc Natl Acad Sci USA*. 1995;92(7):2710-2714. doi:10.1073/pnas.92.7.2710
24. Johnston PJ, MacPhail SH, Banáth JP, Olive PL. Higher-order chromatin structure-dependent repair of DNA double-strand breaks: factors affecting elution of DNA from nucleoids. *Radiat Res*. 1998;149(6):533-542. doi:10.2307/3579899
25. Yokota H, van den Engh G, Hearst JE, Sachs RK, Trask BJ. Evidence for the organization of chromatin in megabase pair-sized loops arranged along a random walk path in the human G0/G1 interphase nucleus. *J Cell Biol*. 1995;130(6):1239-1249. doi:10.1083/jcb.130.6.1239
26. Ostashevsky J. A polymer model for the structural organization of chromatin loops and minibands in interphase chromosomes. *MBoC*. 1998;9(11):3031-3040. doi:10.1091/mbc.9.11.3031
27. Johnston PJ, Bryant PE. A component of DNA double-strand break repair is dependent on the spatial orientation of the lesions within the higher-order structures of chromatin. *Int J Radiat Biol*. 1994;66(5):531-536. doi:10.1080/09553009414551571
28. Gauter B, Zlobinskaya O, Weber KJ. Rejoining of radiation-induced DNA double-strand breaks: pulsed-field electrophoresis analysis of fragment size distributions after incubation for repair. *Rare*. 2002;157(6):721-733. doi:10.1667/0033-7587(2002)157[0721:RORIDD]2.0.CO;2
29. Friedrich T, Scholz U, Elsässer T, Durante M, Scholz M. Calculation of the biological effects of ion beams based on the microscopic spatial damage distribution pattern. *Int J Radiat Biol*. 2012;88(1-2):103-107. doi:10.3109/09553002.2011.611213
30. Friedrich T, Durante M, Scholz M. Modeling cell survival after photon irradiation based on double-strand break clustering in megabase pair chromatin loops. *Radiat Res*. 2012;178(5):385-394. doi:10.1667/RR2964.1
31. Elsässer T, Weyrather WK, Friedrich T, et al. Quantification of the relative biological effectiveness for ion beam radiotherapy: direct experimental comparison of proton and carbon ion beams and a novel approach for treatment planning. *Int J Radiat Oncol Biol Phys*. 2010;78(4):1177-1183. doi:10.1016/j.ijrobp.2010.05.014
32. Hufnagl A, Herr L, Friedrich T, Durante M, Taucher-Scholz G, Scholz M. The link between cell-cycle dependent radiosensitivity and repair pathways: a model based on the local, sister-chromatid conformation dependent switch between NHEJ and HR. *DNA Repair (Amst)*. 2015;27:28-39. doi:10.1016/j.dnarep.2015.01.002
33. Stewart RD, Yu VK, Georgakilas AG, Koumenis C, Park JH, Carlson DJ. Effects of radiation quality and oxygen on clustered DNA lesions and cell death. *Radiat Res*. 2011;176(5):587-602. doi:10.1667/rr2663.1
34. Chatterjee A, Schaefer HJ. Microdosimetric structure of heavy ion tracks in tissue. *Radiat Environ Biophys*. 1976;13(3):215-227. doi:10.1007/BF01330766
35. Kiefer J, Straaten H. A model of ion track structure based on classical collision dynamics. *Phys Med Biol*. 1986;31(11):1201-1209. doi:10.1088/0031-9155/31/11/002
36. Kase Y, Kanai T, Matsufuji N, Furusawa Y, Elsässer T, Scholz M. Biophysical calculation of cell survival probabilities using amorphous track structure models for heavy-ion irradiation. *Phys Med Biol*. 2008;53(1):37-59. doi:10.1088/0031-9155/53/1/003
37. Elsässer T, Cunrath R, Krämer M, Scholz M. Impact of track structure calculations on biological treatment planning in ion radiotherapy. *New J Phys*. 2008;10(7):075005. doi:10.1088/1367-2630/10/7/075005
38. Barkas WH. *Nuclear Research Emulsions: Techniques and Theory*. Academic Press; 1963.
39. Elsässer T, Scholz M. Cluster effects within the local effect model. *Radiat Res*. 2007;167(3):319-329. doi:10.1667/RR0467.1
40. Brons S, Taucher-Scholz G, Scholz M, Kraft G. A track structure model for simulation of strand breaks in plasmid DNA after heavy ion irradiation. *Radiat Environ Biophys*. 2003;42(1):63-72. doi:10.1007/s00411-003-0184-9
41. Thomas CA. The enzymatic degradation of desoxyribose nucleic acid. *J Am Chem Soc*. 1956;78(9):1861-1868. doi:10.1021/ja01590a024
42. Freifelder D, Trumbo B. Matching of single-strand breaks to form double-strand breaks in DNA. *Biopolymers*. 1969;7(5):681-693. doi:10.1002/bip.1969.360070506
43. Hempel K, Mildenberger E. Determination of G-values for single and double strand break induction in plasmid DNA using agarose gel electrophoresis and a curve-fitting procedure. *Int J Radiat Biol Relat Stud Phys Chem Med*. 1987;52(1):125-138. doi:10.1080/09553008714551551
44. Shao C, Saito M, Yu Z. Formation of single- and double-strand breaks of pBR322 plasmid irradiated in the presence of scavengers. *Radiat Environ Biophys*. 1999;38(2):105-109. doi:10.1007/s004110050145
45. Friedrich T, Durante M, Scholz M. Simulation of DSB yield for high LET radiation. *Radiat Prot Dosimetry*. 2015;166(1-4):61-65. doi:10.1093/rpd/ncv147
46. Kundrát P, Friedland W, Becker J, Eidemüller M, Ottolenghi A, Baiocco G. Analytical formulas representing track-structure simulations on DNA damage induced by protons and light ions at radiotherapy-relevant energies. *Sci Rep*. 2020;10(1):15775. doi:10.1038/s41598-020-72857-z
47. Furusawa Y, Fukutsu K, Aoki M, et al. Inactivation of aerobic and hypoxic cells from three different cell lines by accelerated (3)He-, (12)C- and (20)Ne-ion beams. *Radiat Res*. 2000;154(5):485-496. doi:10.1667/0033-7587(2000)154[0485:ioaahc]2.0.co;2
48. Saager M, Glowa C, Peschke P, et al. Fractionated carbon ion irradiations of the rat spinal cord: comparison of the relative biological effectiveness with predictions of the local effect model. *Radiat Oncol*. 2020;15:6. doi:10.1186/s13014-019-1439-1
49. Suzuki M, Kase Y, Yamaguchi H, Kanai T, Ando K. Relative biological effectiveness for cell-killing effect on various human cell lines irradiated with heavy-ion medical accelerator in Chiba (HIMAC) carbon-ion beams. *Int J Radiat Oncol Biol Phys*. 2000;48(1):241-250. doi:10.1016/s0360-3016(00)00568-x
50. Cartwright IM, Su C, Haskins JS, et al. DNA repair deficient Chinese hamster ovary cells exhibiting differential sensitivity to charged particle radiation under aerobic and hypoxic conditions. *Int J Mol Sci*. 2018;19(8):2228. doi:10.3390/ijms19082228
51. Lerch S, Berthold S, Ziemann F, et al. HPV-positive HNSCC cell lines show strongly enhanced radiosensitivity after photon but not after carbon ion irradiation. *Radiother Oncol*. 2020;151:134-140. doi:10.1016/j.radonc.2020.07.032
52. Kalholm F, Grzanka L, Traneus E, Bassler N. A systematic review on the usage of averaged LET in radiation biology for particle therapy. *Radiother Oncol*. 2021;161:211-221. doi:10.1016/j.radonc.2021.04.007
53. Mairani A, Brons S, Cerutti F, et al. The FLUKA Monte Carlo code coupled with the local effect model for biological calculations in carbon ion therapy. *Phys Med Biol*. 2010;55(15):4273-4289. doi:10.1088/0031-9155/55/15/006
54. Inaniwa T, Kanematsu N, Noda K, Kamada T. Treatment planning of intensity modulated composite particle therapy with dose and linear energy transfer optimization. *Phys Med Biol*. 2017;62(12):5180-5197. doi:10.1088/1361-6560/aa68d7
55. Mein S, Kopp B, Tessonnier T, et al. Spot-scanning hadron arc (SHArc) therapy: a proof of concept using single- and multi-ion

strategies with helium, carbon, oxygen, and neon ions. *Med Phys*. 2022;49(9):6082-6097. doi:10.1002/mp.15800
56. Mensour EA, Alam S, Mawani S, et al. What is the future of treatment de-escalation for HPV-positive oropharyngeal cancer? A review of ongoing clinical trials. *Front Oncol*. 2022;12. Accessed August 16, 2023. https://www.frontiersin.org/articles/10.3389/fonc.2022.1067321

SUPPORTING INFORMATION

Additional supporting information can be found online in the Supporting Information section at the end of this article.

How to cite this article: Liew H, Tessonnier T, Mein S, et al. Robustness of carbon-ion radiotherapy against DNA damage repair associated radiosensitivity variation based on a biophysical model. *Med Phys*. 2024;51:3782–3795. https://doi.org/10.1002/mp.17045